

PROCEEDINGS OF SPIE

[SPIDigitalLibrary.org/conference-proceedings-of-spie](https://spiedigitallibrary.org/conference-proceedings-of-spie)

Actuator usage and fault tolerance of the James Webb Space Telescope optical element mirror actuators

A. Barto, D. Acton, P. Finley, B. Gallagher, B. Hardy, et al.

A. Barto, D. S. Acton, P. Finley, B. Gallagher, B. Hardy, J. S. Knight, P. Lightsey, "Actuator usage and fault tolerance of the James Webb Space Telescope optical element mirror actuators," Proc. SPIE 8442, Space Telescopes and Instrumentation 2012: Optical, Infrared, and Millimeter Wave, 84422I (21 September 2012); doi: 10.1117/12.924596

SPIE.

Event: SPIE Astronomical Telescopes + Instrumentation, 2012, Amsterdam, Netherlands

Actuator Usage and Fault Tolerance of the James Webb Space Telescope Optical Element Mirror Actuators

A. Barto, D. S. Acton, P. Finley, B. Gallagher, B. Hardy, J. S. Knight, P. Lightsey
Ball Aerospace and Technologies Corporation, 1600 Commerce Street, Boulder, CO 80301

ABSTRACT

The James Webb Space Telescope (JWST) telescope's secondary mirror and eighteen primary mirror segments are each actively controlled in rigid body position via six hexapod actuators. The mirrors are stowed to the mirror support structure to survive the launch environment and then must be deployed 12.5 mm to reach the nominally deployed position before the Wavefront Sensing & Control (WFS&C) alignment and phasing process begins. The actuation system is electrically, but not mechanically redundant. Therefore, with the large number of hexapod actuators, the fault tolerance of the OTE architecture and WFS&C alignment process has been carefully considered. The details of the fault tolerance will be discussed, including motor life budgeting, failure signatures, and motor life.

Keywords: JWST, cryogenic actuator, motor life, fault tolerance, wavefront sensing, qualification, actuation

1. INTRODUCTION

The primary science requirements for the James Webb Space Telescope (JWST) drove the architecture to include a large aperture (6.5 m diameter) primary mirror. Due to this large required collecting area, the Primary Mirror and Secondary Mirror Support Structure had to be capable of being “folded” for launch and later deployed and phased using images from the flight science cameras. Due to the launch environment and other constraints the eighteen individual primary mirror segments and the secondary mirror are additionally required to be stowed for launch and then deploy to a “nominal” position about which positional adjustments using the rigid body hexapod actuators are made to phase the system. Each Primary Mirror Segment Assembly (PMSA) contains seven gearmotors that are used to drive the six hexapod actuators and the Radius of Curvature (RoC) actuation system. The Secondary Mirror Assembly (SMA) uses six gearmotors to drive its hexapod and there is not a RoC adjustment system on the SMA mirror. All motors used in PMSA and SMA hexapods and RoC adjustment systems are identical in design. While the over-all active architecture of the JWST Optical Telescope Element (OTE) allows a robust solution to manufacturing and alignment tolerances¹, it also represents a mission risk were one or more of the 114 rigid-body hexapod actuators to fail before the telescope is fully phased.

Due to this risk, planned actuator use both on the ground and in flight has been carefully tracked and key decision points are included as part of the Wavefront Sensing & Control (WFS&C) commissioning process for the telescope. This planning and the tolerance of the WFS&C process to the potential of actuator failure was made all the more relevant in June, 2011 when the two gearmotor qualification units both exceeded the pullout current limit of 0.4 amps prior to reaching the 2X life requirement at cryogenic temperatures. This was the second time the JWST gearmotors had failed their life test. While design changes and process improvements have been implemented since the 2011 life test failure that give robust motor performance to

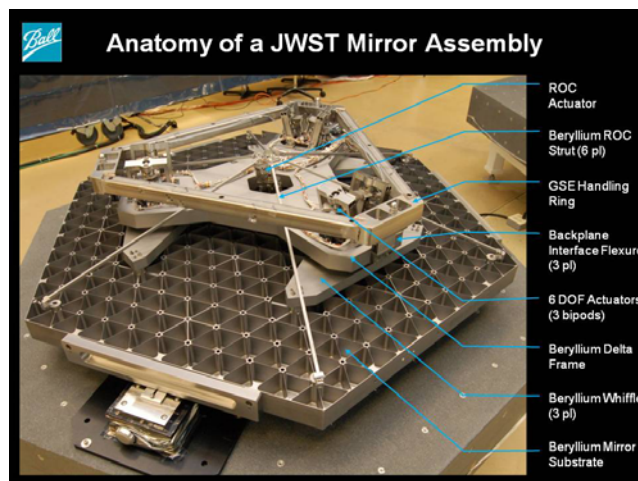


Figure 1 PMSA Components, including actuators

many times the required actuator life, as shown in section 6, the fact remains that limited life resources need to be carefully managed and tracked throughout program development and execution, with fall-back plans and contingencies carefully considered.

2. PREDICTING ACTUATOR LIFE

Actuator bearing failure data was collected on evaluation actuators that were run to failure. In all cases the failure was due to bearing failure. The bearing failures likely had different causative factors, but they all tended to introduce debris into the bearings which ultimately caused the failure. The log-normal distribution function is commonly used to estimate the exponential life expectancy of bearings. This is shown by the typical “bathtub” failure rate plot demonstrated in Figure 2².

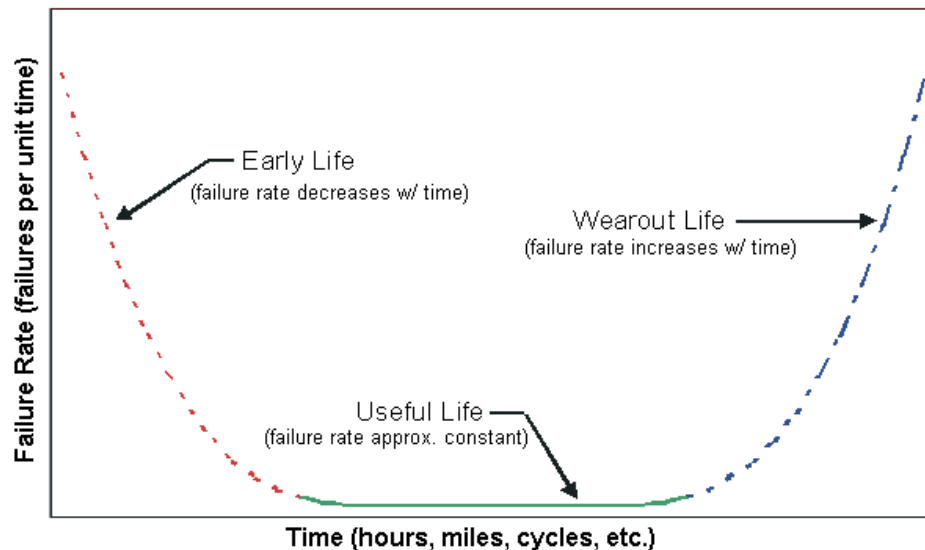


Figure 2 Typical Failure Rate "bathtub" curve

The part of the curve of interest for this paper is the “wearout” rate at the right side of the plot, where a curve is fit starting at the onset of bearing degradation³. The Weibull probability distribution function is characterized by 2 parameters with the most important one being the Beta term since it determines the slope. Given the Weibull distribution, the failure rate can be determined by

$$Failure\ Rate(T) = \frac{B}{n} \left(\frac{T}{n} \right)^{B-1}$$

A series of life tests were conducted on evaluation motors during the course of the failure investigation. In the evaluation motor unit data, onset of failure is determined by an increase in motor drive current. The motors were then driven to failure where in two cases the motors physically failed and in others the motor pull-out current increased excessively indicating the beginning of failure. These motors were not run all the way to failure in order to preserve the motor such that it could be rebuilt with new bearings and used again. In these cases, the motors were driven far enough to allow analytical curve fitting to determine the point at which failure would have occurred. The motor rotation count was recorded for each of those events where they occurred. As will be discussed in section 6, the mechanism for these particular failures was identified and fixed. However, eventual motor failure can be expected to follow this same failure (with onset at a much later point in motor life) and therefore it is informative to study the statistics of the existing failure data. Ten failure cases were examined.

A representative example of motor revolutions versus pullout current data is plotted in Figure 3. The data plotted is after an increase in the current is observed. Three regimes are observed: 1) a linear increase in current; 2) an exponentially increasing portion; and 3) a nearly vertical increase in current in the final stage. In general the number of revolutions a motor exhibited in the linear regime varied greatly. However, the exponential regime was common to all failed motors. For those motors where the tests were terminated before complete failure, an exponential curve was fit over the exponential regime and then projected to a motor current of 0.3 Amps. (The motor in Figure 3 remained in an exponential part of the curve until 0.4 Amps, but more generally 0.3Amps is typical.) The third, vertical regime, from 0.3 to 0.4 was estimated by assuming an additional 21,000 rotations caused the current to exceed the pullout requirement of 0.4 Amps. Pullout current measurement is a quantitative evaluation of torque loss through the motor and gear mechanism. Pullout current greater than the 0.4 amp calculated requirement indicates that the motor has insufficient torque margin to operate. In this way the life expectancy of the 10 failed motors could be compared on a common basis.

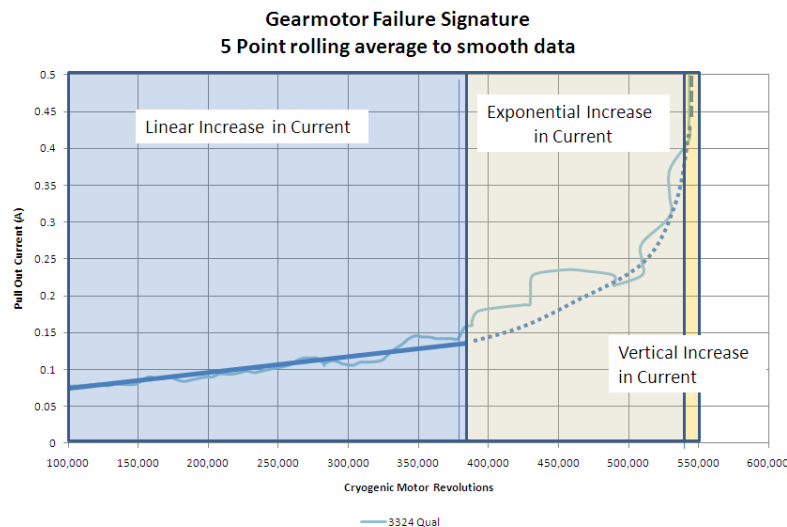


Figure 3 Representative failure data for an evaluation motor. Three regimes were observed in the motor current.

The failure data over the exponential region for the 10 cases were fit to a Weibull distribution as shown in Figure 4. The linear region was based on the 10-case average of 180,000 revolutions.

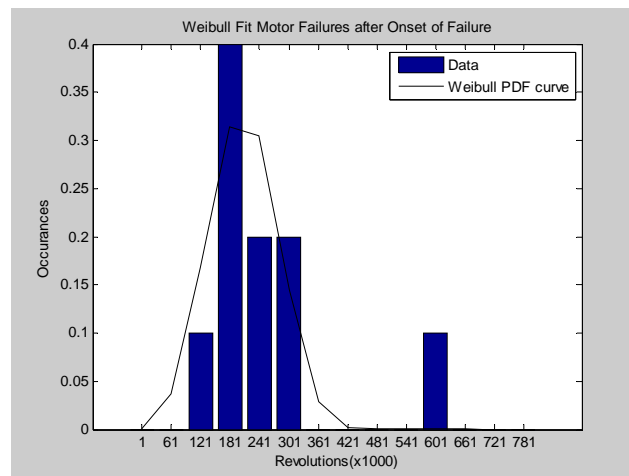


Figure 4 Fit of Weibull curve to experimental motor failures over the exponential region. (Beta = 3.3, eta =232)

The failure rate for a single actuator is plotted as in Figure 5. The 5% chance of a failure for a single actuator is taken from the graph as 97,000 revs + 180,000 linear region = 277,000 revolutions.

Given this model, failure rate probabilities at 5% were estimates for four conditions: 1) any 1 motor failure allowed for the secondary mirror; 2) any 1 motor failure allowed for the 18 primary mirror segments; 3) one combined failure for both the SM and PMSAs; and 4) no failures. A single failure scenario was chosen since after the mirrors deploy a single failure still allows the OTE to be aligned⁴. Table 1 shows the expected revolutions before complete motor failure for these three scenarios. In these scenarios, we calculate the probability estimate for: 1) 5 of the 6 SM motors operating; 2) 107 of 108 PMSA motors operating; 3) 113 of 114 OTE (18 PMSAs + SMA) motors operating; and 4) all 114 motors operating. This allows an estimate of the probability of successful on-orbit commissioning based on the expected needed revolutions. It is assumed in this case that all motors are just below the onset of failure detection. This is a conservative assumption prior to launch.

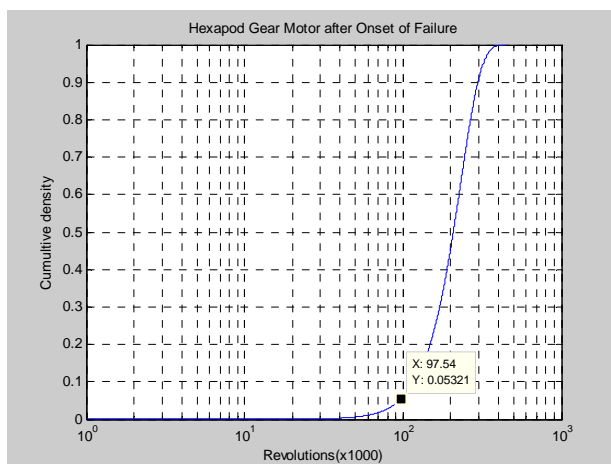


Figure 5 Probability of actuator failure after onset of failure detected after reaching the exponential failure rate. (excludes linear region).

1 SMA Failure	1 PMSA Failure	1 OTE Failure	No Failure
236,000 revs	204,000 revs	203,500 revs	203,000 revs

Table 1 95% probability of success under this scenario

3. ACTUATOR RANGE BUDGETING

The range of six-degree-of-freedom mirror motion required of the active system in order to create an aligned and phased telescope is referred to as “actuator range” (a bit of a misnomer since the actual range needed on each individual hexapod actuator to reach a given mirror pose is not the same as the pose change of the mirror surface). As mentioned above, the individual mirrors are stowed for launch. The nominal deployed position of each mirror defines the mirror control reference frame vertex and the launch-stowed position is defined as an x,y,z position of (0,0,-12.5 mm). As such, the mirror must deploy 12.5 mm to reach its nominal position and then the actuator range needed to reach the phased configuration is defined as further motion about the (0,0,0) coordinate. Actuator range in each degree of freedom is allocated in requirement specifications to account both for known manufacturing and I&T tolerances as well as uncertainties in the ability to measure the as-built configuration of the individual mirror segment during the ground test program. Additionally, range must be available to compensate system-level optical figure and alignment errors. Table 2 below shows the allocated and predicted actuator range needed to cover all these effects.

PMSA/SMA Alignment Tolerances					
Optical Assembly	Value	Piston (mm)	Decenter (mm)	Tilt (mrad)	Clocking (mrad)
PMSA Range Use	allocation	3.29	1.78	1.22	1.70
	prediction	0.81	1.11	0.89	0.97
	margin	309%	60%	37%	75%
SMA Range Use	allocation	3.50	3.50	2.00	N/A
	prediction	1.37	1.63	0.97	N/A
	margin	156%	115%	107%	N/A

Table 2 Actuator range needed to compensate manufacturing alignment and figure tolerances

Budgeting of necessary motor life takes into account these maximum ranges that are expected to be needed to move the mirrors in flight. That being said, not all degrees of freedom are equal in their impact on the ability to create a phased telescope with Image Quality performance within allowable limits. For the PMSAs in particular, clocking and decenter are weak degrees of freedom when compensating low-frequency system error. An example of this can be seen in figure 6 below, showing that the additional residual of choosing to correct 85 nm system-level astigmatism error using only tip, tilt, and piston of the individual primary mirror segments only introduces an additional 4.24 nm rms wavefront error (WFE). Knowing this, were motor life a concern in flight, it would be reasonable to limit the number of motor revolutions applied to moving in the weak degrees of freedom. Indeed, the WFS&C process corrects each degree of freedom independently and reserves compensation via PMSA decentration until later in the process.

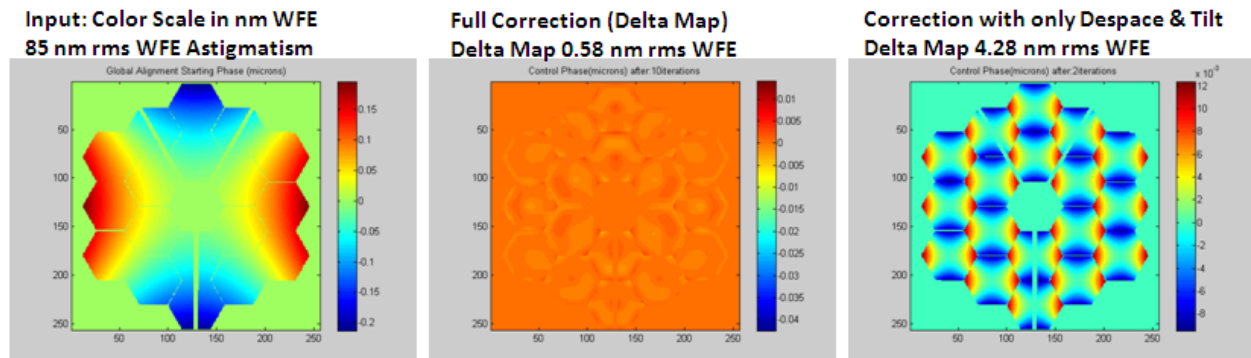


Figure 6 Correction of Global Astigmatism with Full Correction vs. Strong Degrees of Freedom Only

4. ACTUATOR USE BUDGETING

Ultimately, to consider and track motor life, the amount of actuator range needed to deploy and commission the telescope must be tracked in terms of motor revolution steps. The actuator/gearmotor life budget is also used to establish the qualification test parameters to demonstrate the ability of the actuators and gearmotors to survive over 2x the expected lifetime usage. The budget is broken into three main areas: motor life prior to mirror delivery to system I&T; motor life to complete the telescope/Observatory I&T program; and motor usage in flight. As can be seen in the budget summary shown in table 3, 97% of motor life occurs on the ground prior to launch. The number of revolutions seen prior to delivery is based on the worst-case motor usage following mirror-level assembly and optical test and verification plus the expected number of cycles used during the final gearmotor rework operations being performed to retrofit the motors with the new, more robust bearing design discussed in section 6. The number of revolutions allocated to the telescope/system I&T program is based on allocated cycles for integration checkout and ambient temperature mirror testing pre/post environmental testing, as well as a detailed assessment of the

actuators and mirror pose changes defined in the step-by-step plan for cryogenic optical testing to be performed at the Johnson Spaceflight Center (JSC) Chamber A. Each of these expected mirror pose changes was run through the Mirror Control Software (MCS) which is used both during system I&T and in flight to calculate the motor commands necessary to implement a desired mirror pose change. Finally, the in-flight motor use prediction is based on a deployment to the extent of the allocated actuator range and a prediction, by WFS&C commissioning step, for the actuator usage necessary to phase the telescope based on analysis of motor usage during WFS&C commissioning simulation performed during verification of the WFS&C software as described below.

PMSA Hexapod	Gearmotor rev estimate	% of total gearmotor revs	Replacement bearing rev estimate	% of total reworked motor rotor bearing revs
Ambient revs (purged or vac)	956,791	52%	110,091	24%
cryo revs (vac)	821,259	45%	300,339	65%
humidity exposed revs (ambient temp)	66,640	4%	48,440	11%
On orbit cycles consumed	58,772	3%	58,772	13%
Total	1,844,690	100%	458,870	100%
SMA Hexapod	Gearmotor rev estimate	% of total gearmotor revs	Reworked bearing revs estimate	% of total reworked motor rotor bearing revs
Ambient revs (purged or vac)	598,466	42%	88,200	21%
cryo revs (vac)	794,994	56%	310,005	73%
humidity exposed revs (ambient temp)	37,800	3%	28,700	7%
On orbit cycles consumed	62,582	4%	62,582	15%
Total	1,431,260	100%	426,905	100%

Table 3 Actuator/Gearmotor Life Budget

4.1 Actuator Use In Flight and for WFS&C Commissioning

During WFS&C commissioning software verification, a Monte Carlo analysis was performed to run through the full flight commissioning process on an “analytical” telescope deployed to positions and mirror figures consistent with the sub-system level tolerance allocations. As a full run-through of the JWST commissioning software, this analysis included the creation of “mirror update requests” which describe the specific motor moves necessary to implement the mirror pose corrections determined by the WFS&C wavefront analysis software. These mirror update requests were interrogated to determine the number of motor revs used to commission the telescope. The summary of these results is shown in table 4 below.

	Revolutions		
	Max	Min	Mean
PMSA Hex	46314	1241	9738
PMSA Roc	983	11	343
SMA Hex	20352	8633	15007

Table 4 Actuator Revs For Flight WFS&C Commissioning - Monte Carlo Results

This motor rev data was then interrogated by commissioning step to create a flight actuator/motor life budget based upon an assessment of a conservative, allocation-based determination of the number of iterations necessary for each commissioning step and the on-orbit allocation of maximum possible on-orbit alignment range (as described in section 3). In this way the flight allocation of approximately 60,000 revs, as shown in table 3 above, was derived. More details of the flight actuator usage are discussed in section 5.3.3.

5. CONSIDERATION OF FAILURE SCENARIOS

The question of the case of a motor failure during one of the three primary phases of motor usage (prior to subsystem delivery, system I&T, flight deployment and commissioning) must be considered including how to track motor health and the ability to reach an aligned state should the failure occur.

5.1 Prior to Subsystem Delivery

Due to the motor bearing redesign to improve motor life, which occurred after the completion of all other subsystem I&T activities, all motors will have been reworked just prior to delivery to telescope I&T. During the rework process motor pull-out is tracked to a criteria of 37% of the maximum allowable end of life pull-out current defined by torque margin analysis and the reworked bearings see only 150,500 cycles. If the motors show rising pull-out current or other anomalous behavior, they will be reworked until they show the signature of a properly running motor. In this way we are sure of motor health at this point.

5.2 System I&T

During system I&T, motor usage is tracked to ensure the use remains below the allocated 1x life revolutions for each environment (ambient temperature humid, ambient temperature vacuum, and cryogenic temperature vacuum). Per the lubrication life analysis for the dry film lube used in the telescope gearmotor and actuator bearings, humid cycles cause degradation of the lube at a much faster rate than in a dry/purged environment. For this reason humid cycles are the most constrained environment during system I&T. However, the most recent gearmotor life failure showed performance degradation at a significantly greater rate at cryogenic temperatures. Even though the gearmotor bearing design has such been improved, careful attention to the number of cryogenic cycles during system cryogenic test at JSC has been made. Steps already taken to optimize the timeline for the cryogenic test sequence also had the dual purpose of reducing the motor use during the cryo-portion of this test.

In addition to tracking the number of cycles utilized in each environment during I&T, pull-out current will be periodically monitored during this phase of the program. Failures during 2011 qualification testing and subsequent Failure Review Board trouble-shooting activities have shown a consistent signature in rising pull-out current prior to gearmotor failure. Per the earlier discussion in section 2, monitoring the pull-out current level allows early detection and prediction of motor failure.

Pull-out current will be measured using test set electronics during integration testing, pre-/post-vibration test optical testing, and near the completion of cryogenic optical testing at JSC. As shown in section two, the number of motor revs between onset of failure and final failure, for a single actuator, is 277,000 cycles (95% confidence). Given that the total number of motor revs needed to deploy and commission the telescope in flight is < 70,000 for each PMSA and the SMA, if the beginning of a rise in pullout current at the completion of JSC testing is not detected and the motor is allowed to fly, there should still be more than sufficient life remaining in the motor to complete deployment, commissioning, and Wavefront Maintenance throughout the life of the mission.

5.3 In Flight

Motor failure in flight could occur in one of three scenarios: 1) prior to or during mirror deployment, 2) During WFS&C Commissioning, 3) post-initial WFS&C commissioning. The consequence of motor failure on final system performance depends on which phase the telescope is in when the failure occurs.

5.3.1 Motor failure prior to deployment

Failure prior to or during the deployment phase will result in the inability to phase that mirror segment with the rest of the telescope. Were this failure to occur on the SMA, it would be catastrophic to the mission due to the high

sensitivity of OTE focal surface position to SMA despace position. Were the failure to occur on a PMSA motor, the impact to telescope performance is tolerable. The operational plan in this situation is to use the five working hexapod motors and the radius of curvature actuator to adjust the segment in tilt and focus to best align the segment PSF with the PSFs from the other 17 segments. This results in a deterministic PSF that can be deconvolved from the images to mitigate the effect of the un-deployed segment. Prior to deconvolution, the degradation due to an undeployed segment would be on order 11% impact to Strehl and Encircled Energy at 2 micrometers and an 80 milli-arcsecond radius would decrease by approximately 14% for imaging⁵. Figure 7 shows the impact to these terms. While there is a loss of collecting efficiency, the resolution of the PSF is only slightly degraded and the science objectives may be met with minor degradation, primarily in efficiency (integration times to achieve sensitivity goals).

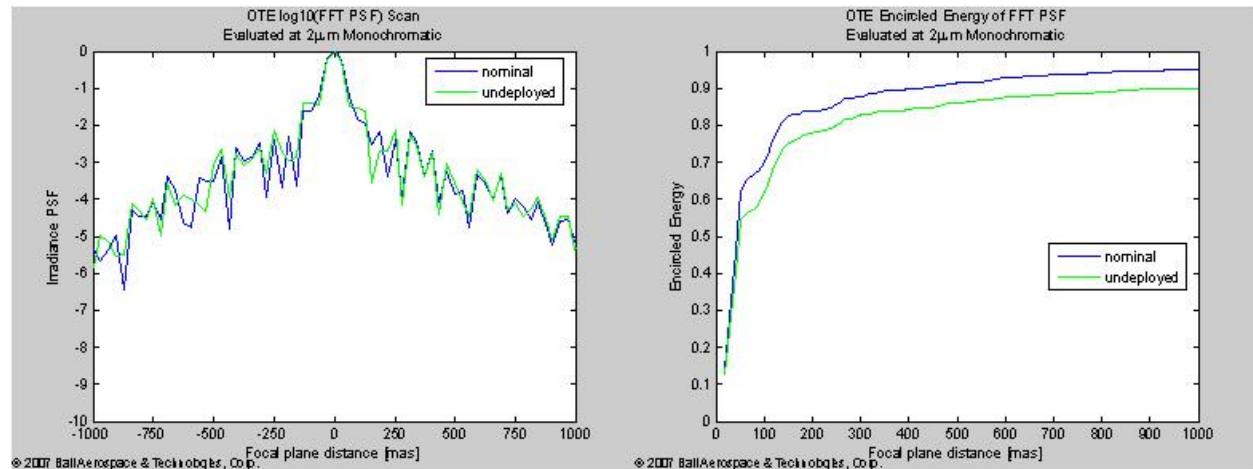


Figure 7 Optical Effect of PMSA Motor Failure Before Deployment

5.3.2 Motor failure during commissioning

At the beginning of WFS&C commissioning, the mirrors are positioned to within 1-2 millimeters of the final aligned position. During commissioning, successive commissioning steps generally consistently improve the state of the telescope with one or two notable exceptions which will be discussed in further detail below. The WFS&C process, described in detail in Reference [6]⁶, is shown in figure 8 below. The commissioning process can be broken up into three primary phases:

- A. **Segment Location and Positioning** – during this preliminary phase, each PMSA image is located and tilt of the segment is adjusted to bring the images into an array on a single NIRCcam detector. Significant SMA piston errors are also corrected in this phase.
- B. **Segment-Level Wavefront Control** – in this phase global alignment allows correction of segment-level alignment errors and correction of PMSA-level astigmatism. The majority of PMSA piston, decenter, and clocking alignment errors will be corrected during this phase. Additionally, the Coarse Multi Instrument Multi Field (MIMF) algorithm uses data across the NIRCcam FoVs to find the best global position for the secondary mirror, adjusting it in decenter and tilt to achieve this alignment. If this step is performed well and the NIRCcam alignment is representative of the global SI/ISIM alignment to the telescope, then the Secondary Mirror should complete this phase very close to its final aligned position. If these assumptions regarding NIRCcam positioning are valid, then following this phase of commissioning, moves larger than a few hundred microns shouldn't be needed during the final commissioning step.

- C. **Global Phasing** – during this final stage of commissioning, the mirrors iterate through image stacking, coarse, and fine phasing to bring the telescope performance from micron-class rms WFE to less than 150 nm rms WFE across the field of view. While there is continued heavy use of the SMA hexapod actuators to create in and out of focus images for use in phase retrieval, actual corrections needed to complete phasing of the telescope during this period should be small unless the SMA position correction made during Coarse MIMF is found to be incorrect when data from all the science instruments is used during MIMF to determine performance across the field of view. If this turns out to be the case, millimeter-class motions of the secondary mirror could be required.

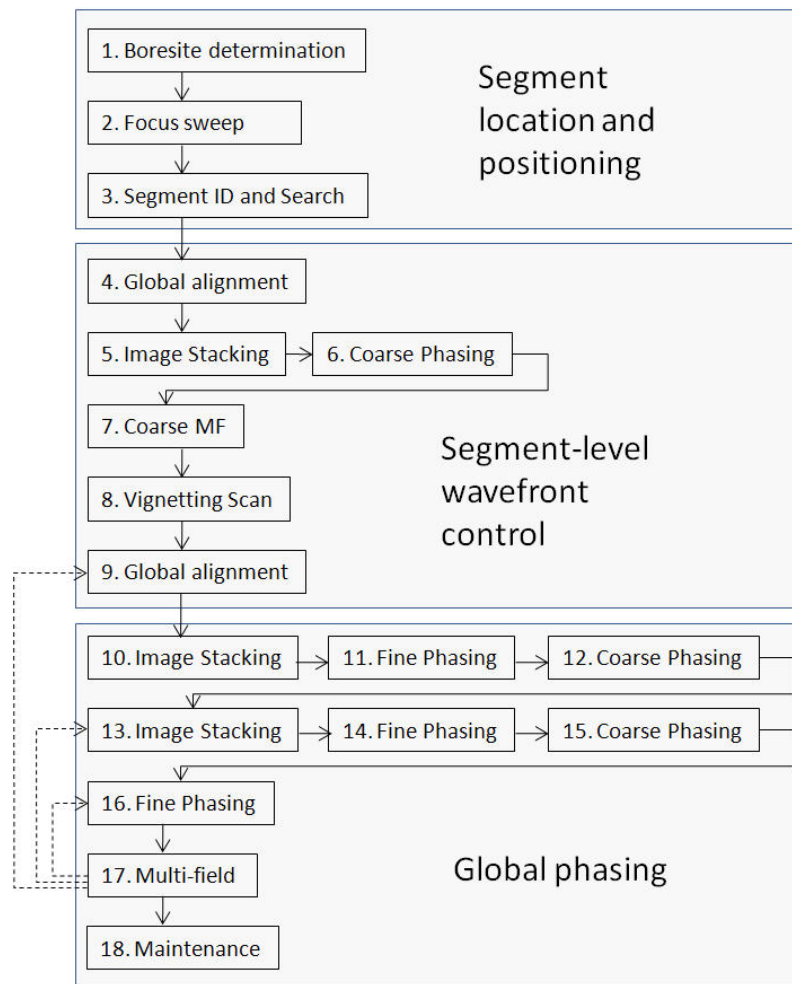


Figure 8 Wavefront Sensing & Control Commissioning Process

The ability to move mirrors sufficiently to phase the telescope with no degradation in optical performance in the presence of a failed actuator is dependent upon how much adjustment is required in order to reach an aligned state, and in what degree of freedom that adjustment must occur. For example, adjusting in tilt with minimal crosstalk into the other degrees of freedom would be more easily achieved than piston or decenter, which would introduce a clocking crosstalk term (which will then be manifested as segment-level astigmatism). Therefore, operational scenarios for a failed actuator will depend how far off the mirror is in each degree of freedom from the ideal. As an example, if a motor were to fail leaving a PMSA off by 1 mm in piston, all the other PMSAs could be adjusted in piston to “meet” it with virtually no impact to telescope. Were a PMSA to fail 1mm off in decenter, the impact to

leaving the segment there would be approximately 100nm additional astigmatism on that segment only, which would degrade telescope performance, for example, from 131 nm rms to 133 nm rms.

It is the location of the Secondary Mirror at the point of a motor failure that has the potential to more significantly impact the performance of the observatory. As mentioned above, following Coarse MIMF in the Segment-Level Wavefront Control phase of commissioning, the SMA has likely been adjusted to within a few hundred microns of its final position and no further large (millimeter-class) motions will be required. Although the commissioning process generally always progresses toward a better aligned system, the Secondary Mirror is purposely moved in piston in and out of alignment many times during the commissioning process in order to create defocused images used to perform phase retrieval in Global Alignment and during MIMF sensing in the science instruments that do not contain weak lenses for WFS&C. This motion is required to assess the state of the telescope and determine the necessary mirror adjustments to complete the commissioning process.

In order to ensure the Observatory is not put in an unacceptable risk position due to the potential of actuator failure at the extreme of one of these SMA piston positions, the ability to move the SMA in a given degree of freedom after actuator failure has been assessed and is shown in the plots below. It should be noted that while it appears analytically possible to move the mirror much further than is shown in the plots below, the additional constraint of maximum allowable stress in the hexapod flexures has been included in this analysis and is the limiting factor on the available stroke in each degree of freedom given an actuator failure. It should also be noted that the ability to move in piston will not be significantly affected even in the case of multiple motor failure on the secondary mirror as long as the failures do not both occur on the same actuator bipod. Finally, as discussed above, movement in the presence of failed actuators will cause a crosstalk into clocking. For the SMA, however, clocking does not affect the over-all performance of the telescope with the exception of possibly needing to make minor adjustments to the PMSA placement to compensate a different clocking orientation of low-order SMA surface errors.

During global alignment, the SMA is adjusted in piston ± 400 micrometers. As can be seen in the upper graph in figure 9, as long as the SMA is within ± 2 millimeters of its nominal deployed position, there is sufficient range with a failure to move the SMA back to its best-focus position. Given that the total range needed to cover all SMA predicted tolerance stack up is less than 2 millimeters (Table 1), even if an SMA motor were to fail when the SMA is in a maximum piston offset position during Global Alignment, it will still be possible to move the mirror back to its best-focus position. This analysis also shows that were a motor to fail prior to putting the SMA in the correct lateral position, there is still sufficient mechanical range with the failed actuator to reposition the SMA as needed.

The other commissioning step that requires large piston of the SMA to support phase retrieval is MIMF, though piston during MIMF is only ± 100 micrometers and therefore clearly at no risk to the ability to reach a phased state. If, however, it is discovered that a large secondary mirror rigid body adjustment could further improve the telescope image quality, careful consideration should be made as to whether it is worth the risk to make a move to that new SM position. Decisions to purposely degrade the performance of a system already at or near required performance levels should never be taken lightly. For this reason, the decision tree shown in figure 10 was developed when the MIMF process was first created to ensure such decisions were made consciously.

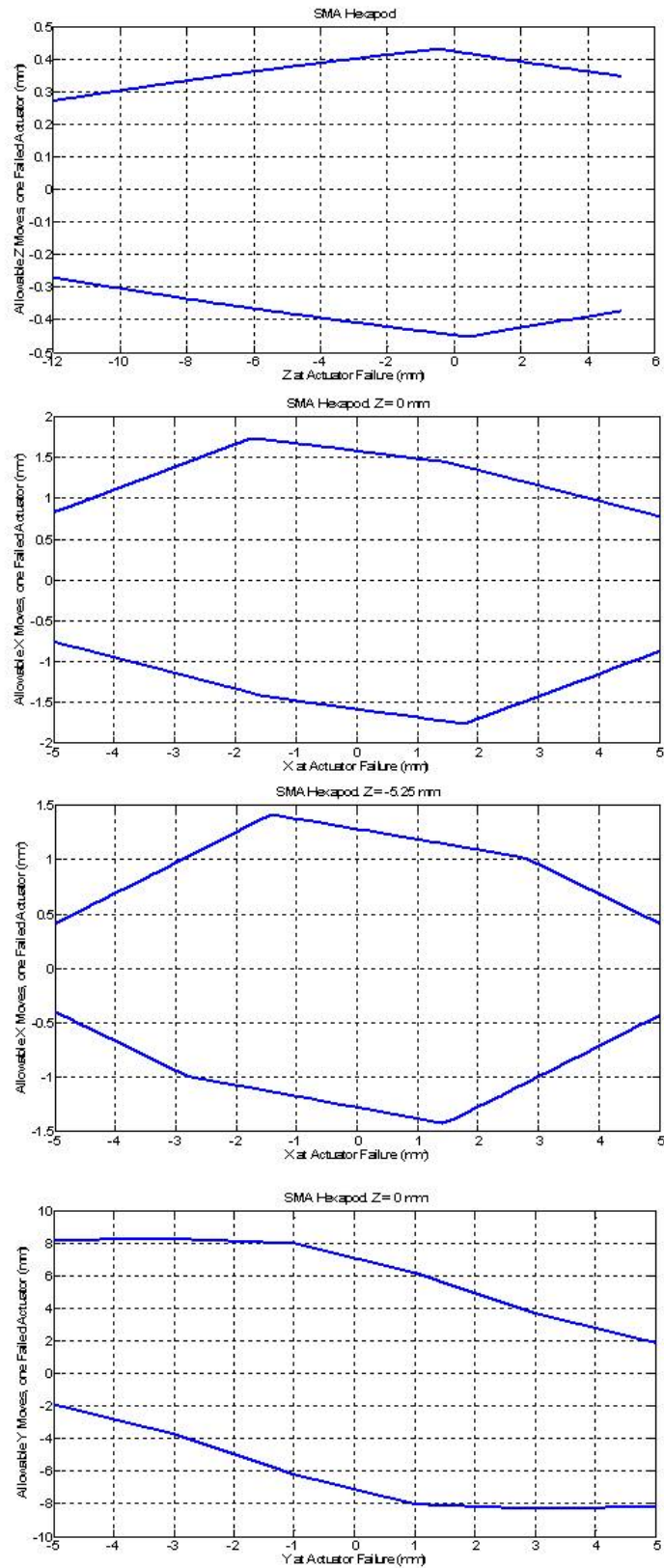


Figure 9 SMA piston and decenter range in presence of motor failure

As this decision tree shows, performance is assessed across the field and instruments are adjusted to best focus to determine if a correction is warranted. If it is determined that a correction is advisable, maximum desired mirror adjustment is considered and, if necessary, limited prior to initiating the correction. This alignment process flow, described in further detail in Reference [1], helps ensure any deviation from the general direction to have mirror position corrections continually improve the state of the system is carefully and consciously considered before the large moves are commanded.

Figure 10 MIMF alignment process decision tree

Commissioning Phase	PMSA	SMA
Total Flight Motor Revs	58,772	62,582
Deployment	22%	23%
Segment Location & Positioning	26%	21%
Segment-Level Wavefront Control	39%	26%
Global Phasing	12%	28%
Maintenance	2%	2%

The analysis to determine the motor usage by commissioning step was created by interrogating Monte Carlo analysis of the flight commissioning process performed using the as-built WFS&C software. In this way, the actual motor revs involved in each segment update request could be explicitly counted. This analysis also was able to determine both the number of motor revs used to perform the sensing operations (such as tilting a PMSA to move from the image array to a single PSF or adjusting the SMA in piston to create defocused images) as well as the expected number of iterations through each algorithm before the telescope reaches the final phased state. This data for the motor revs needed to perform the wavefront sensing observations was combined with the motor revs for the mirror position corrections. The mirror position correction data was collected from multiple Monte Carlo

commissioning study analyses to lend more statistics to the expected mirror use in flight and it is consistent with the requirement-level allocations for in-flight actuator range. In this sense, the motor revolutions required for flight is over stated when compared to the expected flight adjustment ranges shown in table 6

PMSA/SMA Flight Commissioning Range				
Optical Assembly	Piston (mm)	Decenter (mm)	Tilt (mrad)	Clocking (mrad)
PMSA Range Needed in Flight	0.76	0.87	0.84	0.81
SMA Range Needed in Flight	1.08	1.52	0.73	N/A

Table 6 Predicted Compensation Range used during flight WFS&C Commissioning

6. FINAL MOTOR DESIGN – PROCESS & PERFORMANCE IMPROVEMENTS

Over the past ten years of primary and secondary mirror design, build, and test, there have been several design flaws found and corrected in the mirror motors. In all instances of testing the precision cryogenic actuators developed for JWST, it has been the gearmotors that have failed, not the other actuator components which have proven very robust to many times required life. In each case of failure correction, a limited number of motors were tested to prove the design worked to several times the flight motor life requirement, and from the beginning of the program motors have consistently been shown to survive to several million revs. Therefore, the issue in the last two motor failures can be (partially) traced to inadequate process control, which allowed the condition where some motors appeared to work adequately while others failed short of the requirements. A summary of gearmotor design history up to the 2011 Qualification Test failure is as follows:

- 1st Gearmotor Design (4/2004) – Open motor bore, open resolver bore
 - Limited Lube Life Analysis predicts margin over 2X life. (Lube has not been the root cause of any JWST motor failures)
 - Six gearmotors of identical design/processes to flight were each run to between 2.3 million and 12 million motor rotor revolutions
- 2nd Gearmotor Design (5/2007) – Closed motor bore, open resolver bore
 - EDU actuators showed premature degradation due to Teflon in motor bore causing drag
 - Open Bore gearmotors were replaced with new design featuring closed bore
 - Unofficial life test was run on the first closed bore gearmotor received from the vendor – ran over 4 million motor revs
- 3rd Gearmotor Design (5/2009) – Closed motor bore, closed resolver bore
 - Motor in PMSA A1 stopped rotating due to a flake of powder coat in resolver
 - Open resolver gearmotors reworked with vespel sleeve to prevent particulates in resolver windings from entering bore
- 4th Gearmotor Design (2/2010) – Closed motor bore, closed resolver bore, calibrated preload, tighter bearings
 - Qualification test failure in both units traced to front bearing
 - Gearmotors reworked with bearings with reduced radial play and quantified, calibrated bearing preload

Following the 2011 qualification test failure, a Failure Review Board (FRB) was formed with discipline experts from Ball Aerospace, Northrop Grumman, and NASA. Given that this was the the second qualification life test failure, the FRB was particularly methodical in assessment of root cause and agreement on the corrective actions and plan forward. The FRB completed this work between June, 2011 and January, 2012. The failure proved challenging to diagnose due to the sensitivity of the motor bearing design to several process parameters. The final root cause statement identified both the primary root cause, along with many proximate and intermediate causes⁷.

Primary Root Cause Statements

- Inadequate design process for highly sensitive gearmotor bearings (author's note: heritage had been assumed)
- Inadequate process controls for highly sensitive gearmotor bearings

Proximate Cause

- Heritage steel ribbon ball retainer created metallic debris that built up in the raceways and caused premature failure of the bearings during cryogenic operations

Intermediate Causes

- Lubrication Processing Issues Identified:
 - Bearing kits that were matched at the vendor were mixed during the lubrication process
 - When precision matched bearing kits are mixed, the radial play in the bearing is no longer as specified
 - Causes excessively tight radial play in some bearings
 - Low radial play bearings have increased sensitivity to debris
 - Causes front and rear bearings to have different stiffness resulting in increased stress and imbalances in motor
 - Kit mixing can cause multiple ball sizes to be present in a single bearing (100X tolerance)
 - Steel ribbon ball retainer can deform during lubrication process, resulting in potential for interference with inner race
 - Interference potential increases at Cryo due to CTE mismatches between race and retainer

Contributing Factor

- Not accounting for lube thickness, causes un-specified radial play in bearings

During root cause investigation, a new retainer ring was investigated that was both a more robust design (machined crown retainer as opposed to heritage ribbon retainer) and made of PGM-HT material which additionally does not require lubrication for performance at room temperature or cryogenic temperatures. The old ribbon retainer and updated crown retainer designs can be seen in figure 11 below. The PGM-HT crown retainer eliminated many design issues and sensitive processing steps that were part of the ribbon retainer design and in diagnostic testing showed robust performance to many times life even in the presence of some of the processing errors discovered as intermediate causes to the original 2011 qualification failure.



Figure 11 Comparison of heritage ball retainers vs. updated crown ball retainers

After conducting a full gearmotor design review on the updated bearing design and defining several process screening steps to ensure consistent performance across all reworked motors, a two step qualification program was initiated. Phase 1 of the qualification program exposed three gearmotors, installed into actuators, to revolution of 2x life in each environment sequentially, then exposed the qualification units to 7x the required cryogenic revolutions. Upon successful completion of Qualification Phase 1, rework operations on flight motors was initiated. The second phase of qualification testing also used three gearmotors installed into actuators. These motors also saw 2x each environment, but experienced these environments in a more “flight-like” manner, cycling through humid,

ambient vacuum, and cryogenic environments multiple times to represent the I&T flow of the motors. This testing completed in June, 2012. As can be seen in figure 12 below, the performance of the six qualification gearmotors representing the final JWST flight desing and processing show exceptional performance with no sign of degradation even after seeing 7x life. The performance of these motors is in stark contrast to the signature of the two qualification units from the 2011 life test shown on the left section of the plot with exponential current rise similar to figure 3.

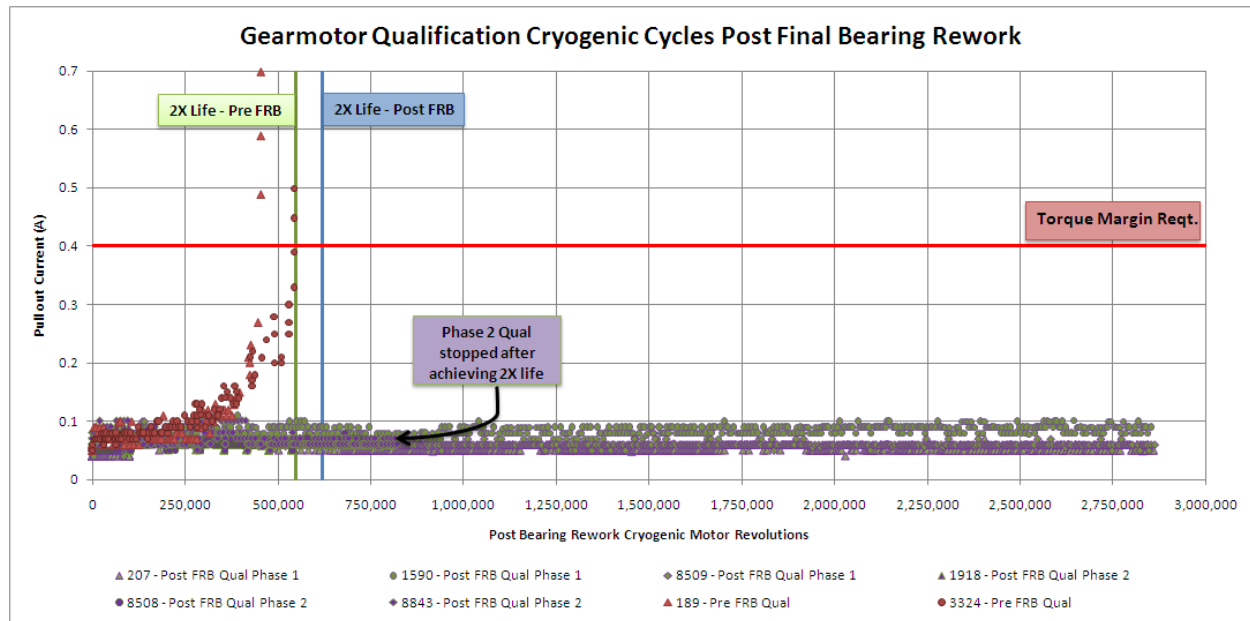


Figure 12 Cryogenic pullout current trend data comparing 2011 vs. 2012 gearmotor design performance

7. CONCLUSION

Although performance of the final PGM-HT crown retainer motor design for PMSA and SMA hexapod gearmotors appears extremely robust, careful planning to monitor the health of this limited resource on the ground and consideration of in-flight failure scenarios is prudent to understanding risk of motor failure on the ability to align and phase JWST in flight. A monitoring program has been established during ground test to understand motor health by periodically recording motor pull-out current and trending over time for each motor. Additionally, steps have been taken to minimize motor use during system I&T. Failure data from the 2011 gearmotor design, which is indicative of bearing failure, has been examined statistically and compared to the expected use of the motors in flight. It has been shown that the number of motor revs between onset of failure and failure is significantly larger than the number of motor revs needed to deploy, commission, and maintain JWST optical performance in flight. Additionally, the effect of motor failure in flight has been considered by program phase and the impacts have generally been shown to be minimal in the case of the PMSAs. For the SMA motors, a failure in flight could be worked around to achieve in-spec alignment in all cases but prior to and during deployment. Finally, large motions of the secondary mirror late in the commissioning process, which would have the effect of degrading system performance before making it better, have been clearly thought out and a flight process decision tree has been implemented to ensure limited resource concerns are considered before these large adjustments are made. All together, this shows a robust fault tolerance program implemented for the JWST Optical Telescope Element.

8. ACKNOWLEDGEMENTS

This effort was supported by the Ball Aerospace & Technologies Corp subcontract with Northrop Grumman Aerospace Systems under the JWST contract NAS6-02200 with NASA Godard Spaceflight Center. The JWST system is a collaborative effort involving NASA, ESA, CSA, the Astronomy community.

REFERENCES

- [1] Knight, J. S, et al., "Observatory Alignment of the James Webb Space Telescope," SPIE 8442-131, these proceedings (2012)
- [2] <http://www.weibull.com/hotwire/issue14/relbasics14.htm>
- [3] Lloyd Schlitzer, "Monte Carlo Evaluation and Development of Weibull Analysis Techniques", ASLE Transactions, Vol. 9, Iss. 4, 1966
- [4] Jessica Gersh-Range, et al, "Minimizing the Wavefront Error Degradation for Primary Mirror Segments with Failed Hexapod Actuators", Opt. Eng. 51, 011005 (2012)
- [5] Knight, J. S. "Effect of Single Segment Failure to Deploy (Maverick Segment), Rev B," JWST Technical Document 06-JWST-0410.
- [6] D. Scott Acton, et. al., "Wavefront Sensing and Controls for the James Webb Space Telescope," SPIE 8442-087, these proceedings (2012).
- [7] Gallagher, Ben, "JWST Gearmotor FRB Final Summary Report," Ball Aerospace & Technologies Corp. JWST Systems Engineering Report (2012).